Cihan University-Erbil Scientific Journal (CUESJ)

Research Article

A Multiband Biconical Log-periodic Antenna for Swarm Communications

Bessam Al Jewad*

Department of Computer and Communication Engineering, Cihan University-Erbil, Kurdistan Region, Iraq

ABSTRACT

In this paper, we present a specific multiband antenna design that addresses the problem of communication with unmanned aerial vehicles (UAVs). We consider a scenario where multiband single-antenna UAV communicates with the rest of the swarm members that are equipped with similar antennas. The key point in the design is that the communication does not require high or low elevation angles in most of the cases. The suggested design has a sufficient degree of freedom to select the desired features for the field pattern while keeping other features such as antenna impedance and gain relatively stable or at least in the acceptable operation region.

Keywords: Biconical antenna, broadband antenna, component, drone-to-drone, drone-to-infrastructure, frequency-independent antennas, log-periodic antenna

INTRODUCTION

In recent years, the use of unmanned aerial vehicles (UAVs), also known as drones, has witnessed an unprecedented increase for both military and civilian applications. From airborne traffic surveillance to the more recent mail package delivery, the list of interesting applications for UAV swarms keeps growing.[1-3] However, the introduction of the swarm concept, communications have always been a challenge.[4,5] In UAV swarms, there are two types of communications: Drone-to-drone (D2D) in which drones can communicate important navigational information between each other, and drone-to-infrastructure (D2I) in which drones can communicate and take general commands from the ground station (GS). While the former can be relatively simple, the latter is much more complicated and challenging for many reasons. First, in most applications, the UAV is equipped with a high-resolution camera sending images and video. Therefore, each UAV requires a high-speed low-latency communication link in the order of tens of Mbps of bandwidth and few tens of milliseconds of latency.[6] That is, of course if such images and videos are to be used for any reliable form of navigation or interaction. Second due to the dynamic nature of the UAV movement in three-dimensional at speeds ranging from 20 m/s to 50 m/s,[6] the communication channel with the GS becomes time varying with non-stationary noise. It is further hampered by the constant loss of the line-of-sight and the change in antenna characteristics (radiation pattern, polarization, etc.) as well as orientation.

Currently, existing wireless technologies, such as wireless fidelity, ZigBee, and XBee-Pro as well as massive multiple-input multiple-output (MIMO) and ultra-wideband communication were devised for communication with UAVs.[6] However, none of these techniques was designed for this particular application making them highly unreliable for many practical situations.[7] In recent artificial intelligence AI studies, it was suggested that navigational information and low-latency interaction or decision-making between the UAV and GS can be minimized if some form of AI algorithm like swarm guidance algorithm was implemented locally on each UAV causing the group to have a massive collective processing power.[8] In such an application, the general heading command can be sent by the GS and the swarm can follow a stochastic general path in which each UAV can communicate the obstacles, constraints and locally-optimized path solution to the rest of the group.[9] Collectively, the group will perform a distributed cost-function minimization and will find the optimal path that minimizes the time and energy for the swarm.[10] In such an application, the design of a special low-cost and ergonomically efficient antenna for D2D communication is highly desirable.

At a basic level, a drone swarm is a floating dynamic wireless network, commonly known as a wireless mesh

Corresponding Author:
Bessam Al Jewad, Cihan University-Erbil, Kurdistan Region, Iraq.
E-mail: bassam.jawad@cihanuniversity.edu.iq.test-google-a.com

Received: Apr 17, 2019
Accepted: Apr 19, 2019
Published: Aug 20, 2019

DOI: 10.24086/cuesj.v3n2y2019.pp85-91

network. A mesh network is a network topology in which each node relays data for the network. All nodes cooperate in the distribution of data in the network. A mesh network whose nodes are all connected to each other is a fully connected network. Many studies suggested the use of multi-carrier, ultra-wideband or multi-band communication. However, one of the limiting factors for such an approach is the antenna.

Many conventional antennas are highly resonant and only operate over a bandwidth that represents a few percent's of their center frequency. These narrow bandwidth antennas may be entirely satisfactory or even desirable for single-frequency or narrowband applications where high gain is required. Wider bandwidths are required in D2D communication applications, especially as the level of the swarm intelligence and its processing power increase. The more sophisticated the applied AI algorithm gets, the more it becomes necessary to exchange high bandwidth or latency dependent data between swarm members. Conventionally, there has been a broad range of work on wideband antennas[11-13] for various airborne vehicle applications. However, D2D rarely will need to communicate at high (or low) elevation angles, especially while flying in a swarm. Therefore, a wideband, omnidirectional antenna, with low beam-width is proposed as a solution for such an application. This antenna needs to be effectively small to maintain the weight constraints of the drone design. In addition, it needs to be a broadband antenna to facilitate exchanging high-bandwidth data.

In this paper, we present a specific antenna design that addresses the problem of multi-band communications and has a higher degree of freedom in its design to select the desired features of the field pattern while keeping other features such as antenna impedance and gain relatively stable or at least within the acceptable operation region.

WIDEBAND FREQUENCY INDEPENDENT ANTENNA

The proposed design is a biconical log-periodic spiral antenna whose conceptual image is shown in Figure 1. The goal is to create a broadband antenna with center frequencies of 3.9 and 5.9 GHz and a frequency range of 3.4–10 GHz. The objective radiation pattern is a one with high gain at the horizon and less gain toward the sky or ground. The reason why an array antenna would not work is that arrays are typically narrow band. Conventionally, several broadband antennas were utilized in the past. However, biconical log-periodic spiral antennas have an advantage in that they can operate in two main modes: The end-fire axial mode with circular polarization and the broadside normal mode with linear polarization. Thus, depending on the operating frequency, they can serve the dual purpose of D2D and D2I communications. This design draws from a range of common antennas including dipoles, arrays, spirals, loops, log-periodic, and conical. The aspects of these antennas and the amount they are used in the design are dependent on the frequency range of operation. In this particular design, the cones are actually present just to support the wire.[14] However, a multi-layered ferrite material can be used inside these cones to adjust the center frequency and change the polarization. As will be shown later each part of a loop will have a different center frequency, and since Ferrite material is narrow band, in general, a multi-layer stack of ferrite materials can be utilized depending on the desired characteristics from the antenna. The material around the core can be filled with dielectrics to enhance the capacitive effect of the antenna impedance to adjust the performance.

In general, a broadband antenna is defined by two factors: Percentage of center frequency and ratio of operation. The percentage of the center frequency is defined by

$$F_p = \frac{f_u - f_l}{\sqrt{f_l * f_u}} \times 100\% = \frac{f_u - f_l}{f_c} \times 100\% \quad (1a)$$

while the frequency ratio of operation is defined as the ratio of the upper and lower frequencies of operation f_u and f_l.

$$F = \frac{f_u}{f_l} \quad (1b)$$

If the impedance and the pattern do not change significantly over about an octave ($F=2$) or more, we classify the antenna as a broadband antenna. To meet the frequency independence requirements in a finite structure, the current must attenuate along with the structure and be negligible at the point of the truncation. For radiation and attenuation to occur the charge must be accelerated (or decelerated) and this happens when the conductor is curved or bent normally to the direction, in which the charge is traveling. Thus, the curvature of the spiral provides a frequency-independent operation over a wide bandwidth.[12]

Broadly speaking, each arm of this antenna can be designed independently and placed strategically to provide a set of electrically small loop antenna array elements spaced by half wavelength, and excited at the center. Starting from one arm the logarithmic (log) spiral is defined in cylindrical coordinates by $r=\alpha^{\theta}$ or $\ln(r)=\theta \ln(\alpha)$ and is shown in detail in Figure 2. The radial distance to a point p on the spiral is r, the angle with respect to the X-axis is θ, and α is a constant representing the apex angle. The relationship between θ and r can alternatively be given by $\theta=\tan(\beta) \ln(r)$.

In both relations, the z is not specified. An important control for a log-periodic spiral angle is the relationship for the spacing between each loop.[15] To achieve the broadband nature, the ratio between the i^{th} loop spacing s and the subsequent loop must stay constant. The log-periodic loop array seems a reasonable approximation to the spirally wrapped wire in our design. The loop diameters increase along with the antenna so that the included angle α is a constant and the spacings s of adjacent elements are scaled. This can also be translated in terms of the height of the loop z, which gives:

$$\frac{S_{i+1}}{S_i} = \frac{z_{i+1} - z_i}{z_i - z_{i-1}} = k \quad (2)$$

where k is some constant. From this equation, it can be easily seen that z follows a simple difference equation.

Since the arrangement is logarithmic, it is more convenient to let $z=m^{\theta}$. Now to find the height of each loop z_i we will assume that completes one full rotation for each discrete loop and is therefore an integer i times 2π. Thus, the height of the

i^{th} loop can be written as $z_i = m^i$. Therefore, $z_{i+1}=m^{(i+1)}=mz_i$ in the same way $z_{i+1}=m^2\ z_{i-1}$. Substituting this in (2) and solving for m, we find that $m=k$ for a non-trivial solution and therefore $z=k^\theta$.

It is fairly reasonable to assume that only a single loop (or part of the loop) from the spiral will contribute to the major far-field component and will have the major current distribution according to the frequency of interest. This assumption was validated by several simulations. In this sense, the diameter for any element n+1 is approximately k^n greater than the first element, or

$$\frac{D_{n+1}}{D_1} = F \approx k^n \tag{3}$$

where F is the frequency ratio from Equation (1); the smallest loop in the antenna has a circumference equal to a tenth of a wavelength to quantify for the small loop antenna definition which gives the constraint for the diameter of the first loop. Therefore, the geometric representation for one arm of the biconical antenna is given by

$$r=e^{q/\tan q}, z = k^q \tag{4}$$

Equations (3) and (4) constitute the design equations for one arm of the antenna. Each antenna arm can be placed in either a frequency selective biconical construct shown in Figure 1 or stacked in a broadband uni-conical construct.

MULTI-BAND ANTENNA MATCHING

In the previous section, the antenna was designed to meet several broadband requirements. In general, most self-complementary broadband antennas have almost constant impedance. The problem with most wire antennas (like our design) is that the antenna impedance is highly frequency dependent. Thus, even though the antenna arm in the previous section may have broadband properties, it can only be used with a single frequency dictated by the matching network. The alternative would be to utilize a broadband matching network and in this case, the matching would not be perfect or easy. In addition, broadband matching in general means a compromise on the antenna gain due to the constant gain-bandwidth product constraint.

Using the design equations of the previous section, the parameters selected for our design are shown in Table 1. The simulation results for the antenna impedance assuming a wire gauge of AWG33 are shown in Figure 3 for an input port impedance of 50 Ohm.

The approach that was adopted in our matching is the dual-band impedance matching where the antenna is matched at 3.9 GHz and 5.9 GHz. The same approach can be expanded to match any set of frequencies within the band. In this section, the approach is introduced. Analyzing the actual antenna response on the Smith Chart (from a vector network analyzer) is also performed.

The antenna's frequency response (that is, the reflection coefficient Γ) is plotted as a function of frequency on the Smith Chart, as shown in Figure 4. The blue curve in this Figure 4 represents the antenna impedance, plotted on the Smith Chart

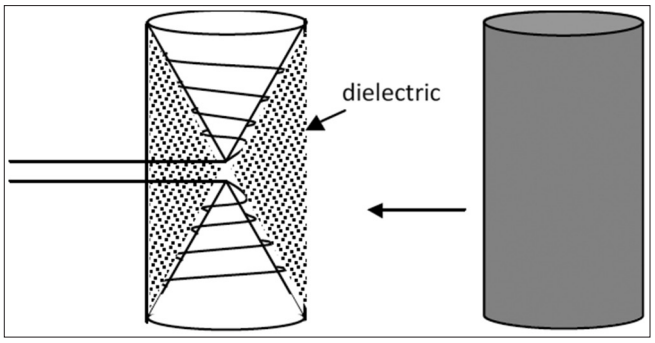

Figure 1: Proposed antenna concept

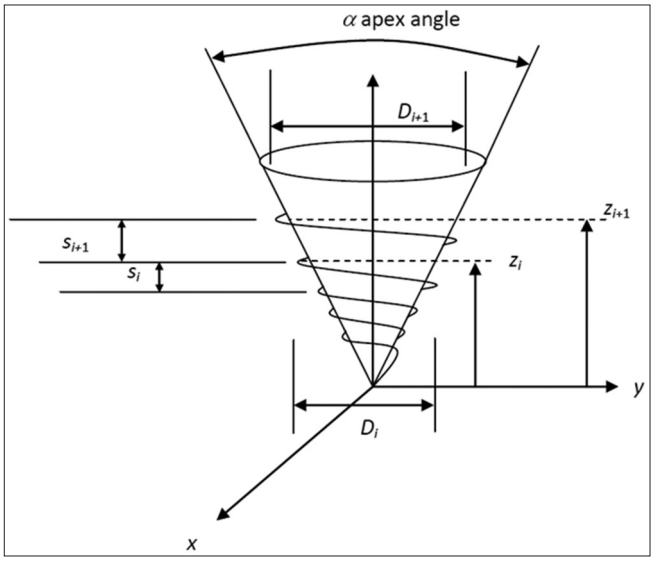

Figure 2: Log-periodic loop array structure

Table 1: Design parameters for the initial antenna matching circuit

Parameters	Values
Circumference	≤λ/10
Low frequency	3.481 Ghz
Large frequency	10 Ghz
β	1.54 radians
K	1.235
Radius of wire	0.0899 mm
Number of turns	5

continuously from 3.4 GHz to 6.2 GHz since the rest of the frequency response is not required for the matching. The black circles indicate the locations on the curve corresponding to 3.9 GHz–5.9 GHz.

The corresponding VSWR plot for the same impedance above is given in Figure 5.

The target is to bring both of the above impedance locations to the center of the smith chart with a single matching network. To do this, the low band is matched first. For this step, use is made of only series capacitors and parallel inductors. This is because series capacitors affect lower

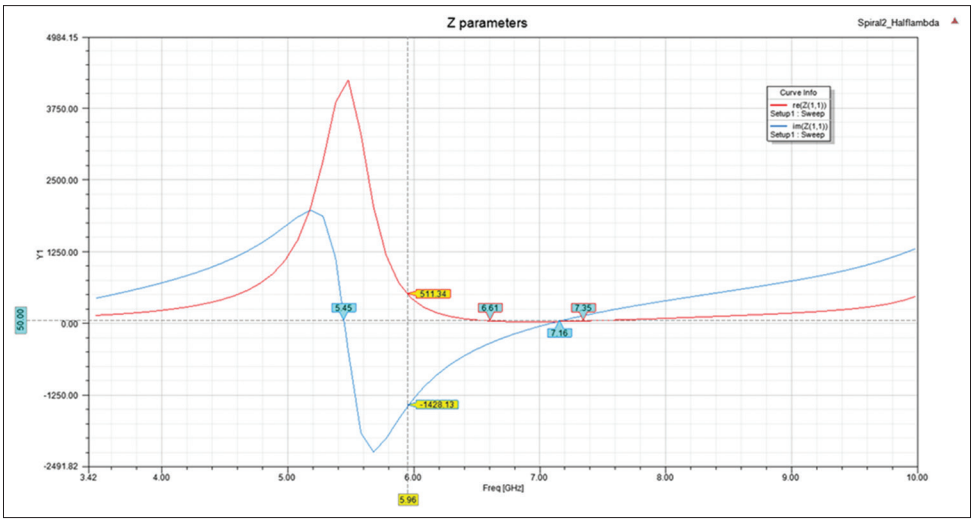

Figure 3: Un-matched antenna impedance

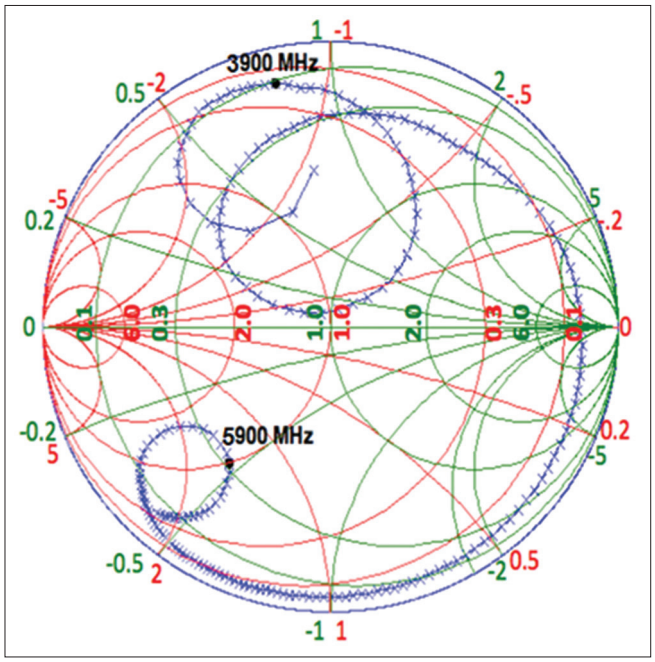

Figure 4: Antenna reflection coefficient frequency response

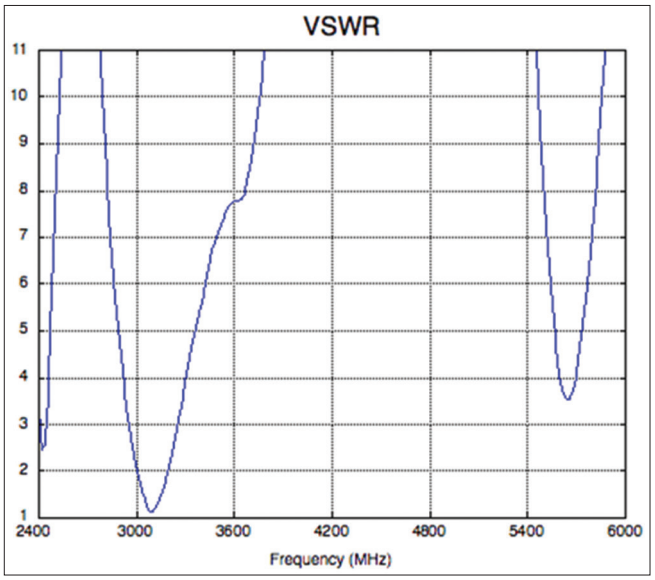

Figure 5: Original VSWR for the antenna

frequencies more than higher frequencies. Similarly, parallel inductors affect low frequencies more than high frequencies. As a result, if only those components are used, the low band can be matched with minimal effect on the high band. The matching is done by calculating the required series and parallel impedances by moving on a constant X circle on the immittance Smith Chart.

For the lower band matching a series, capacitor will move the impedance to intersect the Re[y]=1 circle. By inspection, we find that a 0.738 pF series capacitor will move the 3.9 GHz impedance to intersect the Re[y]=1 circle. From there, we complete the low band match with a parallel inductor of approximately a 0.692 nH. The resulting impedance curve for the group (the antenna, the 0.738 pF series capacitor and then the parallel 0.692 nH inductor) is shown in Figure 6.

From this, we see that the low band (3.9 GHz) is moved to the center of the Smith Chart, i.e., we have impedance matched in this region. However, the high band (5.9 GHz) region has moved from its original location, even though that was not intentional. The next step is to try to match the 5.9 GHz point without undoing the 3.9 GHz match. This can be done with the use of parallel capacitors and series inductors (both of which affect high frequencies more than low frequencies). To this end, we want to swing the high band point in Figure 5 into the center of the Smith Chart. Using the concepts of the parallel capacitor, we can move the 5.9 GHz impedance to intersect the Re[z]=1 circle through a 0.483 pF parallel capacitor. Note that by doing so, the 3.9 GHz point is moved slightly away from the center but that can be tolerated. The high band is now set up to be matched with a series inductor. The required value can be found to be approximately 1.61 nH of series inductance. The addition of this component to the overall matching network produces the final impedance curve, as shown in Figure 7.

From Figure 7, the high and low bands may not appear exactly matched. However, Figure 8 presents the VSWR corresponding to the impedance plot of the above Smith chart. At 3.9 GHz and at 5.9 GHz, the VSWR is <2.0. This is typically considered a good match. If a better match was desired, the four component values could be further optimized to improve the response. The trick to optimize for the component values is to assume that each value has a correction factor of δ. From the location of each desired point, we can determine the sign and value of each δ. The key factor to remember if lumped elements are to be used is the parasitic of each element.

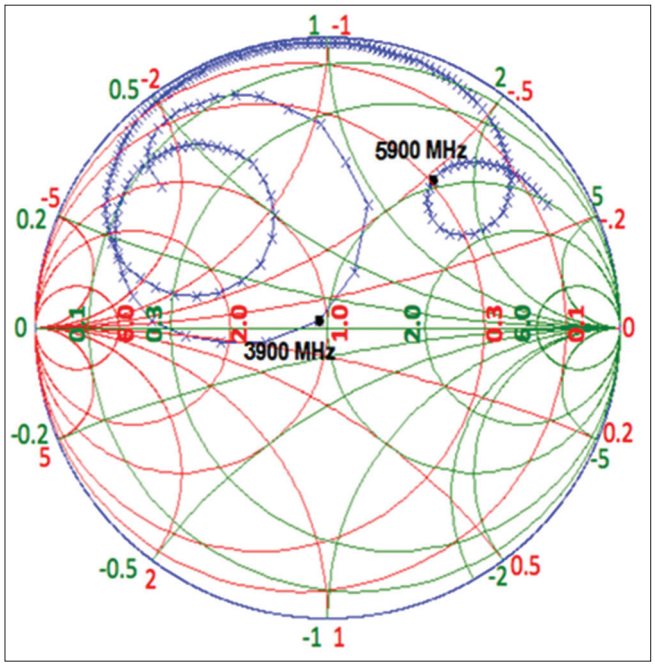

Figure 6: Matching of the lower frequency band

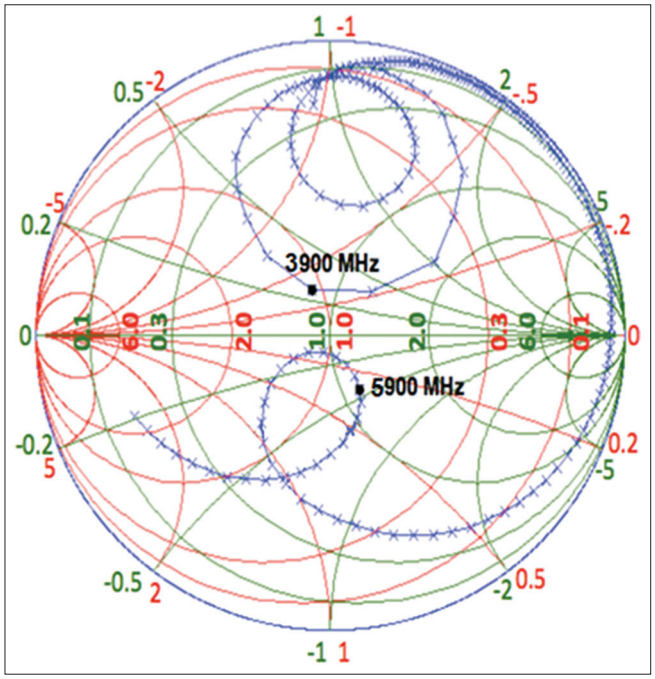

Figure 7: Matching of the upper frequency band

The final step in our matching is to convert the lumped elements found into short-embedded transmission lines, as shown in Figure 9. The reason for this step is that lumped passive elements rarely behave as pure elements at very high frequencies. For example, a simple inductor will be hampered by stray capacitance and by wire resistance converting it into a more complicated circuit element, and the same applies to capacitors. In addition, the values we found for the matching network are not very practical.

Thus, the initial lumped-element values found were converted to distributed elements by utilizing the theory of embedded short transmission line.[16] In general, a short-embedded transmission line can approximate a shunt capacitance or a series inductance.

As long as the length of the transmission line is kept very small compared to the minimum wavelength of interest, the implementation is possible. Other examples exist in[16] for more complicated matching networks, and the selection between different possible matching networks depends entirely on the practicality of the element dimensions.

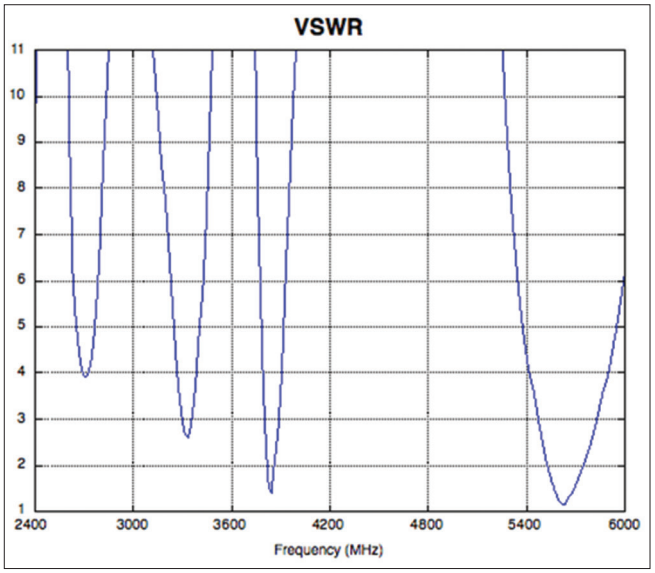

Figure 8: VSWR for the matched antenna

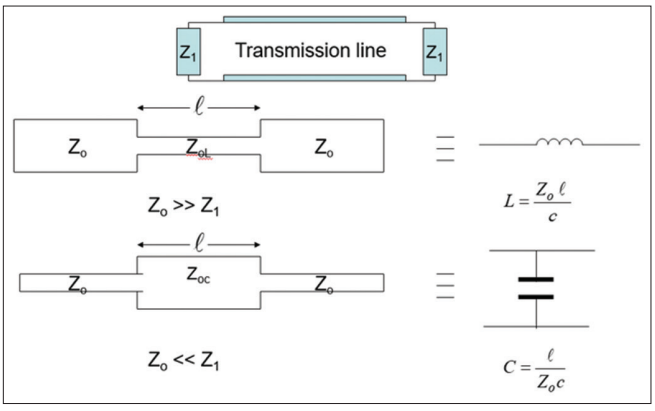

Figure 9: Short-embedded transmission line implementation of the matching network

Figure 10: Actual implementation of the matching circuit

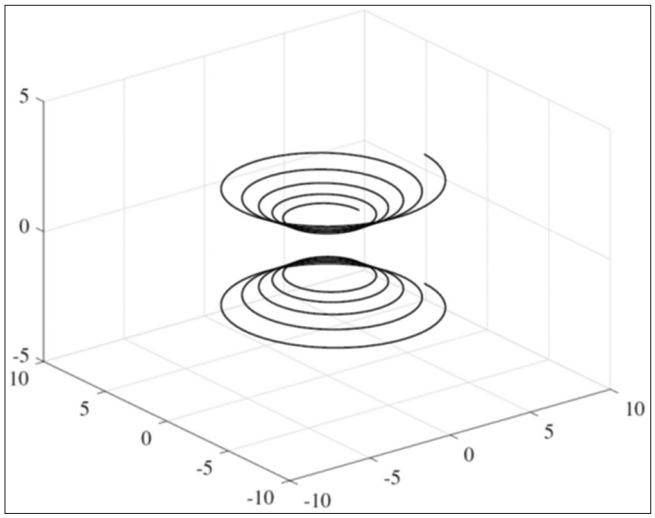

Figure 11: The biconical log-periodic spiral antenna (dimensions are in mm)

The resulting overall matching network was implemented on a Rogers 4350B substrate, as shown in Figure 10 for the entire frequency band.

SIMULATION RESULTS

The resulting antenna design from the previous section for a biconical construct is shown in Figure 11. This design had been simulated with Ansoft HFSS. The separation between the two conic sections was selected to give resonance at the 3.9 GHz–5.9 GHz. The S_{11} or reflection coefficient is shown in Figure 12 and the radiation pattern for the 5.9 GHz is shown in Figure 13 for 5.9 GHz. The reflection coefficient response is <-10 dB over the entire band of interest and the center frequencies of 3.9 GHz–5.9 GHz have very apparent resonant peaks. This is due to the wideband nature of the spiral antennas. As was devised previously, only part of each loop contributed to the radiation pattern in each frequency. The rest of the stacked loops aided in increasing the broadside gain to 5 dBi by working as a reflector and helping to limit the beam width at high and low elevation angles at the center frequency by working as a guide.

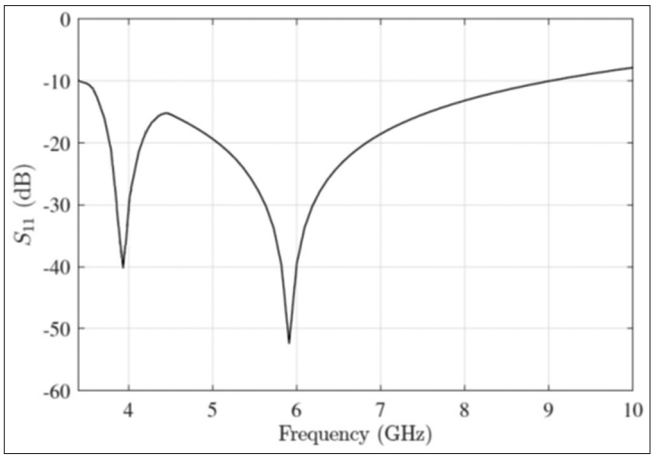

Figure 12: Simulated reflection coefficient or S_{11} (dB)

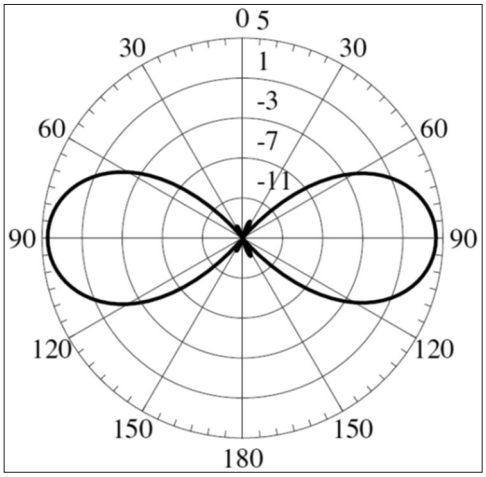

Figure 13: Radiation pattern of antenna (dBi)

CONCLUSION

This paper studied a broadband biconical log-periodic antenna design for UAV communications. A geometrical analysis of the design is presented along with an HFSS simulation.

The results show that this antenna has good performance at the proposed frequency range with center frequencies at 3.9 GHz and 5.9 GHz. The results show that this antenna can achieve a gain of 5 dBi. Further work will focus on increasing the gain and miniaturizing the antenna size using ferrite stacks and proper dielectric materials.

REFERENCES

1. S. Hayat, E. Yanmaz and R. Muzaffar. "Survey on unmanned aerial vehicle networks for civil applications: A communications viewpoint". IEEE Communications Surveys and Tutorials, vol. 18, no. 4, pp. 2624-2661, 2016.
2. T. Andre, K. A. Hummel, A. P. Schoellig, E. Yanmaz, M. Asadpour, C. Bettstetter, P. Grippa, H. Hellwagner, S. Sand and S. Zhang. "Application-driven design of aerial communication networks". *IEEE Communications Magazine*, vol. 52, no. 5, pp. 129-137, 2014.
3. J. Abatti. "*Small Power: The Role of Micro and Small UAVs in the Future*". Air Command and Staff College, Maxwell AFB, AL, 2005.

4. P. Olsson, J. Kvarnstrom, P. Doherty, O. Burdakov and K. Holmberg. "Generating UAV communication networks for monitoring and surveillance". In: Proceeding International Conference on Control Automation Robotics Vision, pp. 1070-1077, 2010.
5. E. Yanmaz, R. Kuschnig and C. Bettstetter. "Achieving air-ground communications in 802.11 networks with three-dimensional aerial mobility". In: Proceeding IEEE INFOCOM, pp. 120-124, 2013.
6. P. Chandhar, D. Danev and E. G. Larsso. "Massive MIMO for communications with drone swarms". *IEEE Transactions on Wireless Communications*, vol. 17, no. 3, pp. 1604-1629, 2018.
7. A. Pospischil and J. P. Rohrer. "Multihop routing of telemetry data in drone swarms". In: Proceeding of ITC, 2017.
8. M. V. Ramesh, P. L. Divya, R. V. Kulkarni and R. Manoj. "A Swarm Intelligence Based Distributed Localization Technique for Wireless Sensor Network". Proceeding International Conference on Advances in Computing, Communications and Informatics, pp. 367-373, 2012.
9. L. Rosenberg. "Artificial Swarm Intelligence vs Human Experts". International Joint Conference on Neural Networks, 2016.
10. C. Papagianni, K. Papadopoulos, C. Pappas and N. D. Tselikas. "Communication Network Design Using Particle Swarm Optimization". Proceeding International Multiconference on Computer Science and Information Technology, vol. 3, pp. 915-920, 2008.
11. V. Rumsey. "Frequency independent antennas". *IRE International Convention Record*, vol. 5, pp. 114-118, 1957.
12. J. D. Kraus. "Helical beam antennas for wide-band applications". *Proceeding of the IRE*, vol. 36, no. 10, pp. 1236-1242, 1948.
13. Y. Mushiake. "Self-complementary antennas". *IEEE Antennas and Propagation Magazine*, vol. 34, no. 6, 1992.
14. J. Dyson. "The unidirectional equiangular spiral antenna". *IEEE Transactions on Antennas and Propagation*, vol. 7, no. 4, pp. 329-334, 1959.
15. J. D. Kraus and R. J. Marhefka. "*Antenna for All Applications*". McGraw-Hill, New York, 2002.
16. B. C. Wadell. "*Transmission Line Design Handbook*". Artech Print on Demand, Boston, 1991.